Published in final edited form as:
Neuron. 2008 August 14; 59(3): 439–449. doi:10.1016/j.neuron.2008.05.026.

Neurotransmitter modulation of small conductance Ca^{2+}-activated K^+ (SK) channels by regulation of Ca^{2+} gating

François Maingret[1], **Bertrand Coste**[1], **Jizhe Hao**[1], **Aurélie Giamarchi**[1], **Duane Allen**[2], **Marcel Crest**[1], **David W Litchfield**[3], **John P. Adelman**[2], and **Patrick Delmas**[1,†]

1*Centre de Recherche en Neurobiologie et Neurophysiologie de Marseille (CRN2M), CNRS UMR 6231, Université de la Méditerranée, Boulevard Pierre Dramard, 13916, Marseille Cedex 20, France.*

2*Vollum Institute, Oregon Health and Science University, Portland, Oregon 97329, USA.*

3*Department of Biochemistry, Siebens-Drake Research Institute, University of Western Ontario, London, Ontario, Canada.*

Summary

Small-conductance Ca^{2+}-activated K^+ (SK) channels are widely expressed in neuronal tissues where they underlie post-spike hyperpolarizations, regulate spike-frequency adaptation and shape synaptic responses. SK channels constitutively interact with calmodulin (CaM), which serves as Ca^{2+} sensor, and with protein kinase CK2 and protein phosphatase 2A, which modulate their Ca^{2+} gating. By recording coupled activities of Ca^{2+} and SK2 channels, we showed that SK2 channels can be inhibited by neurotransmitters independently of changes in the activity of the priming Ca^{2+} channels. This inhibition involves SK2-associated CK2 and results from a 3-fold reduction in the steady-state Ca^{2+} sensitivity of channel gating. CK2 phosphorylated SK2-bound CaM but not KCNQ2-bound CaM, thereby selectively regulating Ca^{2+} gating of SK2 channels. We extended these observations to sensory neurons by showing that noradrenaline inhibits SK current and enhances signaling of primary afferent neurons in a CK2- dependent fashion. Hence, neurotransmitter-initiated signaling cascades can dynamically regulate Ca^{2+} sensitivity of SK channels and directly influence somatic excitability.

Introduction

The small conductance, Ca^{2+}-activated potassium (SK) channels are found in both neuronal and non-neuronal tissues (Köhler et al., 1996; Bond et al., 1999). Three homologous SK channels, SK1–3, are expressed in the mammalian brain and display partially overlapping distributions (Stocker et al., 1999). In many neurons throughout the nervous system, SK channels regulate firing frequency by contributing to medium afterhyperpolarization (mAHP) that follows action potentials (Bond et al., 2004; 2005; Storm et al., 1990), although other ion channels, including M/KCNQ- and h-channels, also contribute to mAHPs (Gu et al., 2005). SK channels are also important in regulating dendritic excitability (Cai et al., 2004), synaptic transmission and plasticity (Ngo-Ahn et al., 2005; Faber et al., 2005; Hammond et al., 2006).

†Correspondence should be addressed: Centre de Recherche en Neurobiologie et Neurophysiologie de Marseille (CRN2M), CNRS UMR 6231, IFR Jean Roche, Faculté de Médecine, Université de la Méditerranée, Boulevard Pierre Dramard, 13916, Marseille Cedex 20, France. Phone: +33 4 91 69 89 70, Fax: +33 4 91 69 89 77, E-mail: patrick.delmas@univmed.fr.

Indeed, SK2 channel plasticity contributes to the increased EPSP underlying long-term potentiation (LTP) (Lin et al., 2008) and facilitates hippocampus-dependent learning and memory (Hammond et al., 2006; Stackman et al., 2002).

SK channels are activated by low concentrations of intracellular Ca^{2+} ions (EC^{50} of ~0.3–0.5 μM; Köhler et al., 1996) and sense Ca^{2+} via binding of Ca^{2+} ions to calmodulin (CaM), which is constitutively bound to the C terminus domain of the channel (Xia et al., 1998; Keen et al., 1999). Recent evidence also indicate that native SK2 channel complexes are comprised of the protein kinase CK2, a ubiquitous serine/threonine protein kinase, and the protein phosphatase 2A (PP2A) (Bildl et al., 2004), which serve opposing roles in regulating Ca^{2+} gating of SK2 channels (Allen et al., 2007). The central role of these enzymes in regulating the Ca^{2+} sensitivity of SK channels suggests that Ca^{2+} channel-independent pathways might modulate SK channel functions by tuning their Ca^{2+} gating.

Here, we provide evidence that SK channels can be modulated by transmitters, independently of change in Ca^{2+} channel activity, through CK2 and PP2A mediated modulation of their apparent Ca^{2+} sensitivity. Hence, neurotransmitters can dynamically regulate Ca^{2+} sensitivity of SK channels and directly influence spike-frequency adaptation of peripheral and central neurons.

Results

Activation of SK channels in response to the opening of single Cav2.2 channels

We first recorded coupled activities of endogenous Ca^{2+} and SK channels using perforated outside-out microvesicles pulled-out from somatic membranes of sympathetic superior cervical ganglion (SCG) neurons (Fig.1a). Single channel activities were elicited by stepping from –70 to 0/+5 mV. Out of 12 microvesicles recorded, only 2 contained SK-like channel activity, suggesting that native SK channels are not homogeneously distributed on the cell surface of SCG neurons.

To increase the probability of obtaining Ca^{2+} and SK channel coupling, cDNA coding for rSK2 channels was intranuclearly microinjected into SCG neurons and unitary currents were recorded 2 days later. In these experiments, only microvesicles containing a single channel activity with resolved openings were used. A representative recording of the combined activation of an endogenous Cav2.2 channel together with a SK channel is shown in Fig.1c. With external Ca^{2+} and K^+ set at 20 and 10 mM respectively, single channel conductances for Cav2.2 and SK channels were 16.8 ± 1.2 pS (n = 6) and 8.9 ± 0.9 pS (n = 9). The SK channel conductance recorded here was very similar to that of rSK2 expressed in oocytes (Hirschberg et al., 1998). Ca^{2+} channel activity was abolished by ω-conotoxin GVIA (500 nM, n = 5; Fig. 1b) whereas activity of SK was fully blocked by apamin (300 nM, n = 7, Fig. 1c). SK channels activated ~3 ms after the onset of the Cav2.2 current and peaked < 19 ms after peak I_{Ca} (inset in Fig. 1c). On average, SK channel activated with a time constant of 12.9 ± 1.6 ms in response to the opening of a single Cav2.2 channel (n = 7). This is in good agreement with previous studies on rSK2 expressed in oocytes (Hirschberg et al., 1998;Köhler et al., 1996), predicting time constants of activation of 20 ms and 6.3 ms in response to 1 and 10 μM intracellular Ca^{2+}, respectively. SK channel activity was not detected when no Ca^{2+} channel was present in the microvesicle or when Ca^{2+} channels were blocked by ω-CgTx GVIA (n = 4, Fig. 1d).

Neurotransmitter-induced modulation of SK channels is independent from Ca^{2+} channel inhibition

Applying noradrenaline (NE, 1 μM) inhibited both Ca^{2+} and SK channel activities in 75 % (9/12) of microvesicles tested (Fig.1d). Taking the change in the peak of pseudomacroscopic

currents as an index for inhibition (Fig.1d), Cav2.2 and SK currents were reduced by 64 ± 4 % (n = 5) and 57 ± 5 % (n = 4), respectively. We presume that the appropriate adrenergic receptor(s)/transducing pathway(s) were lacking in the unresponsive microvesicles.

Cav2.2 channels are inhibited by Gβγ following NE application (Ikeda, 1996), and therefore it is unclear whether it is the Ca^{2+} channel or the SK channel *per se*(or both) that are the target (s) for modulation. We therefore replicated the above experiments in neurons pre-injected with cDNA coding for the rat Cav2.3 channel subunit (α1E, rbEII) with a short N-terminal sequence (GenBank: L15453), that is not inhibited by Gβγ (Bourinet et al., 1996; Page et al., 1998). Activation of Ca^{2+} channels was then recorded 2 days later in the presence of ω-CgTx GVIA (500 nM) and nifedipine (1 μM) to block endogenous Cav2.2 and Cav2.1 channels, respectively. Ca^{2+} channels recorded under these conditions could be activated by stepping from a holding potential of −70/−80 but not from −40 mV (n = 9), consistent with the inactivation properties of Cav2.3 channels. NE (1 μM) reduced whole-cell Cav2.3 currents by only 11 ± 2.8 % (n = 9, see Fig. 4a) whereas ≥ 60 % inhibition was typically observed for whole-cell Cav2.2 currents in sympathetic neurons (Ikeda, 1996; Delmas et al., 2000). Accordingly, NE did not cause a significant change in single Cav2.3 channel activity when tested using perforated microvesicles (2–6 % reduction in charge transfer; Fig.2a). Although Cav2.3 channels displayed faster inactivation than Cav2.2 when Ca^{2+} was used as a charge carrier, they could promote activation of SK2 channels (Fig. 2b,c). However, it should be noted that the rate of activation of SK2 channels was slower (τ = ~23 ms) than with Cav2.2 channels, possibly reflecting a smaller rise in Ca^{2+} at the vicinity of the SK channel (Fig.2c).

The activity of Cav2.3-driven SK2 channels was strongly inhibited by bath application of NE (1 μM) (Fig. 2b,c). Inhibition took 10–40 s to develop, plateaued within 4–5 min and reversed within 6–13 min (Fig. 2d) and was best prevented by a cocktail containing the α_1- and β-adrenergic receptor antagonists, prazosin (3 μM) and timolol (5 μM) (n = 5). On average, pseudomacroscopic SK currents were inhibited by 69.3 ± 7 % compared with only 12.5 ± 4 % for Cav2.3 currents (Fig. 2e).

We next examined whether other neurotransmitters exhibited the ability to modulate SK currents. We found that somatostatin (Sst, 500 nM) inhibited SK currents by 32 ± 6 %, whereas bradykinin (BK, 200 nM) and angiotensin II (AGII, 500 nM) caused no significant inhibition of SK currents (Fig. 2e). Despite its inability to modulate SK current AGII produced stronger inhibition (22 ± 6 %) of Cav2.3 currents than Sst and BK (11–13 %; Fig. 2e).

Transmitter modulation of SK channels results from reduced Ca^{2+} sensitivity of channel gating

To examine whether the apparent Ca^{2+} sensitivity of SK2 channels is altered during neurotransmitter action, steady-state SK2 channel activity was recorded in microvesicles 'artificially' loaded with different concentrations of free Ca^{2+} using ionomycin (1–3 μM) added to the patch pipette solution (Fig.3). When microvesicles were loaded with 1 μM Ca^{2+}, NE reduced mean p_o from 0.64 ± 0.06 to 0.27 ± 0.07 (n = 5) (Fig. 3a1). In contrast, NE had little detectable effect on SK2 channel activity in microvesicles loaded with 3 μM free Ca^{2+} (n = 7) (Fig.3a2). Under these conditions, SK2 channels exhibited a high p_o of 0.71 ± 0.08, which was not altered by NE. This observation suggested that change in the Ca^{2+} gating of SK channel by Ca^{2+}-bound CaM could be responsible for the agonist action. Consistent with these results, steady-state $[Ca^{2+}]_i$-response curves for SK channels showed that the apparent EC_{50} value was shifted rightward from 0.42 ± 0.06 to 1.37 ± 0.1 μM in the presence of NE (Fig. 3b).

CK2-mediated phosphorylation of calmodulin is involved in SK channel modulation

To test whether CK2-mediated phosphorylation of SK2-associated CaM is involved in the change of apparent EC_{50}, steady-state Ca^{2+} dose-response relationships were determined in the continued presence of the specific CK2 inhibitor 4,5,6,7-Tetrabromo-2- azabenzimidazole (TBB). Activation curves determined in 10 μM TBB-treated microvesicles yielded an apparent EC_{50} value of 0.30 ± 0.05 μM (Fig. 3c, n = 6) in agreement with Allen et al., (2007). The presence of TBB strongly reduced the effect of NE since steady-state $[Ca^{2+}]_i$-response curves in the presence of NE yielded an EC_{50} value of 0.39 ± 0.08 μM (Fig. 3c).

The predominant form of the CK2 enzyme is a heterotetrameric complex consisting of two catalytic α subunits and two regulatory β subunits (Litchfield, 2005). We compared the Ca^{2+} sensitivity and modulation of SK2 channels in neurons overexpressing the wild-type CK2β/CK2α holoenzyme with those in neurons expressing a site-directed mutant of the catalytic subunit of CK2α that is kinase inactive (CK2αK68M) (Penner et al., 1997; Vilk et al., 1999). SK2 channels co-assembled with the CK2β/CK2α holoenzyme showed slightly reduced Ca^{2+} sensitivity compared to SK channels in neurons expressing CK2β alone (EC_{50} values of 0.69 ± 0.08 and 0.49 ± 0.06 μM, respectively) (Supplemental Fig.1). The rather modest decrease in Ca^{2+} sensitivity of SK channels in cells overexpressing CK2β/CK2α suggested that SK channels were subjected to tonic protein phosphatase activity. Consistently, expression of CK2β/CK2α in conjunction with treatment with okadaic acid (200 nM for 1 hr), a specific inhibitor of PP1 and PP2A, increased the EC_{50} value to 0.89 ± 0.09 μM (n = 4, data not shown). The Ca^{2+} sensitivity of SK channels assembled with the kinase dead CK2β/CK2αK68M was 0.38 ± 0.08 μM (n = 13; Fig. 3d). Upon co-expression of SK2 with CK2β/CK2αK68M, NE failed to change the Ca^{2+} response relationship significantly, with an EC_{50} value of 0.43 ± 0.07 μM (Fig. 3d).

To test whether modulation was mediated by SK2-associated CK2, we expressed the site-directed K121A mutant of SK2, which has been shown to suppress SK2-bound CK2 activity (Allen et al., 2007). The apparent Ca^{2+} sensitivity of K121A mutants was left-shifted to 0.36 ± 0.08 μM, consistent with tonic regulation of SK2 channel Ca^{2+} sensitivity by CK2 and PP2A. NE failed to change significantly the Ca^{2+} response relationship of SK2 K121A channels, yielding an apparent EC_{50} of 0.39 ± 0.09 μM (Fig. 3e). In addition, the EQRK to AQAA SK2 mutant, which exhibits greatly diminished ability to bind PP2A (Allen et al. 2007), had a Ca^{2+} sensitivity shifted to the right (EC_{50} = 0.71 ± 0.05 μM). Consequently, the effects of NE were partly occluded with an apparent EC_{50} for Ca^{2+} of 0.98 ± 0.09 μM (Fig. 3e, n = 5; $P<0.05$). These data support the idea that NE effects occur through SK2-associated CK2 phosphorylation and that SK2-associated PP2A tonically opposes these effects.

CK2 phosphorylates CaM complexed with SK2 but not KCNQ2 channels

To determine whether NE phosphorylates SK2-associated CaM, we performed immunoprecipitations using a specific SK2 antibody (Fig. 3f). Two days after transfection of fetal SCG cell cultures, [$^{32}P_i$] metabolically labeled cells were analyzed by immunoprecipitation, western blotting and radiolabeling. Immunocomplexes precipitated by the SK2 antibody contained low levels of ^{32}P-CaM (Fig. 3f). NE markedly enhanced ^{32}P-CaM associated with SK2, whereas preincubation with TBB prevented this effect (Fig. 3f,g). Specificity was monitored by parallel experiments in which we tested whether NE promotes the phosphorylation of CaM when complexed with KCNQ2 (Kv7.2) subunits (Delmas and Brown, 2005;Yus-Nájera et al., 2002;Wen and Levitan, 2002). The results presented in the bottom panel of Fig.3f show that CaM precipitated from Flag epitope-tagged KCNQ2 immunocomplexes was not phosphorylated, suggesting that NE phosphorylated CaM in a CK2-dependent manner only when CaM was complexed with SK2 channels.

To further demonstrate the essential role of CK2 phosphorylation of CaM in NE-mediated changes in Ca^{2+} sensitivity of SK channels we co-expressed SK2 with a site-directed mutant of CaM (CaMT80A), which prevents CK2 phosphorylation (Bildl et al., 2004) (Fig. 4a). Calcium concentration response relationship of CaMT80A-associated SK2 channels provided an EC_{50} value of 0.37 ± 0.08 μM (Fig. 4b). NE did not significantly affect the Ca^{2+} sensitivity of SK2 channels assembled with CaMT80A (EC_{50} = 0.45 ± 0.09 μM, n=7) (Fig. 4b).

Modulation of SK2 channels reduces AHP and spike-frequency adaptation

We next examined the potential for noradrenergic modulation of SK-mediated whole-cell currents using the amphotericin B-perforated patch method. Figures 5b1–b4 show representative recordings from SCG neurons co-expressing Cav2.3 and SK2 subunits, in which Nav and M/KCNQ K^+ channels were blocked by TTX (200 nM) and linopirdine (10 μM), respectively. Linopirdine, up to 200 μM, has been shown to have no effect on rSK2 (Dreixler et al., 2000). Under these conditions, bath application of NE produced a slow decrease in peak outward tail currents (I_{AHP}) evoked by brief depolarizing voltage step to 0 mV (Fig. 5b1). Similar results were obtained in the 8 cells tested, with a mean inhibition of 71 ± 8 % (Fig. 5c,d). Application of apamin (100 nM) blocked I_{AHP}, thus identifying it as SK current, and prevented further inhibition by NE (Fig. 5b2). NE inhibition was reduced to 35 ± 6 and 27 ± 7 % in TBB-treated cells and CK2β/CK2αK68M-expressing cells, respectively (Fig. 5c,d).

The implication of CK2 was confirmed using 2 new ATP site-directed inhibitors of CK2, chosen among the most effective and selective compounds, namely 1,8-dihydroxy- 4-nitroanthracene-9,10-dione (MNA) and 8-hydroxy-4-methyl-9-nitrobenzo[g]chromen-2- one (NBC) (Meggio et al., 2004). One hour pre-incubation of cells with MNA and NBC reduced NE inhibition of I_{AHP} to 28 ± 6 and 26 ± 6 %, respectively (Fig. 5d). These values are qualitatively the same as those for TBB and CK2β/CK2αK68M.

In some neurons, SK channels contribute to the mAHP that follows action potentials (APs) (Maylie et al., 2003; Faber and Sah, 2007). Therefore, we investigated how NE affected AHP in the absence of linopirdine in neurons coexpressing Cav2.3 and SK2 subunits. Figure 5e illustrates the changes that NE produces on the AHP that follows a single AP elicited at ~-60 mV with a brief current injection. NE markedly reduced the amplitude of the AHP in control neurons whereas TBB and expression of CK2αK68M greatly impeded NE action (Fig. 5e,f). On average, NE reduced AHP peak amplitude from 21.7 ± 2 to 15.4 ± 1.4 mV ($P < 0.01$) in control neurons, and from 21.8 ± 1.6 to 19.5 ± 1.5 mV ($P > 0.05$) and 19.4 ± 1 to 17.8 ± 0.9 mV ($P > 0.05$) in neurons treated with TBB or expressing CK2β/CK2αK68M, respectively (Fig. 5f).

Noradrenergic modulation of native SK channels in nociceptive DRG neurons

Recently, SK channels have been shown to play a key role in controlling sensory pathways including nociceptive inputs into the spinal cord (Bahia et al., 2005). In sensory dorsal root ganglia (DRG), SK1 and SK2 are preferentially expressed in small nociceptive DRG cells, whereas SK3 is expressed both in small and large cells (Bahia et al., 2005; Mongan et al., 2005). Therefore, we tested whether NE, which has pronociceptive actions, regulates native SK channels and spike-frequency adaptation in putative nociceptors (Fig. 6). We examined NE responses in cultured small DRG neurons expressing Cav2.3 and bathed with ω-CgTx GVIA (200 nM), nifedipine (1 μM), ω- agatoxin IVA (200 nM) and amiloride (250 μM) to block endogenous Ca^{2+} currents (Coste et al., 2007). Application of NE for 2 min caused an increase in the number of APs elicited by current step injection, which was associated with the suppression of the AHP, essentially mimicking the effects of apamin (Fig. 6a). We quantified the effects of NE on excitability by examining the relationship between injected current and AP firing. NE increased by 1.5– to 3-fold the number of APs elicited over a range of injected

current amplitudes (Fig. 6b). We confirmed that NE had no significant effects on either Cav2.3 or KCNQ/M currents recorded in such cells (Fig. 6c1,c2), but inhibited apamin-sensitive K^+ currents evoked by repolarizing voltage steps or ramps (Fig. 6c3,c4). One hour pre-incubation of DRG cultures with MNA (1 μM) reduced NE inhibition of I_{AHP} from 41 to 14 % (Fig. 6d). Most of the cells responding to NE were found sensitive to capsaicin (Fig. 6e).

Discussion

We have used perforated microvesicles from SCG neurons in order to simultaneously record coupled activities of Ca^{2+} channels and heterologously expressed SK2 channels, and to study their regulation by neurotransmitters. We demonstrated that Ca^{2+} influx produced by the activation of either Cav2.2 or Cav2.3 channels permits a sufficient rise in intracellular Ca^{2+} to open expressed SK2 channels. Although we over-expressed SK2 subunits, SK3 and possibly SK1, are natively expressed in rat SCG neurons (Hosseini et al., 2001) and can potentially form multimeric channels with SK2 (Monaghan et al., 2004; Strassmaier et al., 2005). Therefore, it is possible that some heteromeric channels are formed. Nevertheless, our findings provide the first evidence that neurotransmitter-generated second messengers, independent of their effects on Ca^{2+} channels, can directly modulate SK2-containing channels. Thus, under conditions where Cav2.3 channels showed little inhibition through adrenergic and somatostatinergic receptors, SK2 channel activity was markedly reduced. There are precedents for the inhibition of SK channels by α_1- and β-adrenergic receptors in neurons of the preoptic area (Wagner et al., 2001) and by somatostatin in medium spiny neostriatal neurons (Galarraga et al., 2007), although it was not investigated whether inhibition was direct or subsequent to Ca^{2+} channel modulation. Direct inhibition of SK channel activation by the sigma receptor type 1 (σR-1) was recently demonstrated in CA1 pyramidal cells of rat hippocampus (Martina et al., 2007). Inhibition of the SK current in both SCG and DRG neurons caused a reduction in the afterhyperpolarization (AHP) and spike frequency adaptation. NE inhibition of SK channel activity in sensory neurons may be a mechanism underlying NE-induced ectopic firing and sympathetically maintained pain (Pertovaara, 2006).

Structural, proteomic, and functional studies have shown that the SK2 channel complex contains the SK2 pore-forming subunits of the channel as well as constitutively bound CaM that acts as the Ca^{2+} sensor for the channels, and additionally contains CK2 and PP2A. In this complex, CK2 phosphorylates SK2-bound CaM at threonine 80 and reduces the effective Ca^{2+} sensitivity of the channels. SK2-bound PP2A antagonizes the effects of CK2 phosphorylation. Therefore, although SK2 channels are gated solely by intracellular Ca^{2+} ions, they are multiprotein signaling complexes (Xia et al., 1998; Bildl et al., 2004; Allen et al., 2007) in which the Ca^{2+} sensitivity of the channels may be tuned in response to metabolic signals and thereby alter the SK2 channel effects on membrane potential. Our data show that the NE-induced inhibition of SK2 channel activity resulted from a threefold reduction in the steady-state Ca^{2+} sensitivity of SK2 channel gating, and that the decreased Ca^{2+} sensitivity is due to NE-initiated signals that dynamically regulate CK2 phosphorylation of SK2-bound CaM. Importantly, we showed that NE promoted the selective CK2-mediated phosphorylation of SK2-bound CaM, while sparing KCNQ/M-channel-bound CaM. This provides a likely explanation for the absence of regulatory actions of NE on KCNQ channels (Gamper and Shapiro, 2003). Moreover, the results show that even for a ubiquitously and highly expressed signaling molecule such as CK2 that maintains an overall standing activity, exquisite specificity may be endowed by the macromolecular composition of CK2-containing multimeric complexes (Bildl et al., 2004; Allen et al., 2007) and/or their organization into distinct membrane microdomains (Delmas and Brown, 2002; Delmas et al., 2002).

Our data show that NE may not result in global CK2 activation or mobilization of already active CK2, but rather selective targeting of SK2-bound CK2. In this regard, the CK2

holoenzyme is virtually inactive on CaM but can be activated by positively charged molecules, such as polylysine and polybasic proteins (Arrigoni et al., 2004). Allen et al., (2007) have recently demonstrated that the N-terminal domain of SK2 contains a cluster of positively charged residues, and that lysine 121 (K121) activates CK2 to phosphorylate SK2-bound CaM, only when the channels are closed. This state-dependence of CK2 activity to SK2-bound CaM mediated by K121 suggests that the NE-induced regulation of SK2 channels by CK2 may be affected by conformational changes that alter the relative position of K121 within the SK2 channel complex. While it is clear that NE inhibits SK2 channel activity by selectively influencing SK2-bound CK2, the signal from the activated receptor to CK2 within the SK2 channel complex is not yet known. An attractive possibility is that NE signals, possibly through phosphorylation of the intracellular terminal domains of SK2 that contain multiple protein kinase acceptor sequences, by a distinct protein kinase to alter the relative proximity of the K121 to CK2, thereby promoting phosphorylation of SK2-associated CaM.

SK channels are activated by elevations of intracellular Ca^{2+} and exert a local repolarizing, inhibitory influence on the membrane potential that affects membrane excitability and in many cases this results in attenuation of Ca influx. Our results show that in DRG neurons NE modulation of SK channel activity via CK2 influences somatic excitability, and this may be a general mechanism in many central neurons where SK2 channels contribute to the AHP that follows an action potential. In addition, emerging roles for SK2 channels have been described. For example, in hippocampal pyramidal neurons, SK2 channels in the dendrites collaborate with Kv4 channels to shape and limit the time course of local Ca^{2+} plateau potentials (Cai et al., 2004). In CA1 (Ngo-Anh et al., 2005) and amygdala (Faber et al., 2005) pyramidal neurons, synaptically evoked Ca^{2+} influx through NMDAr activates closely coupled SK channels in the postsynaptic density, which reduces the magnitude of the AMPAr mediated depolarization thereby shaping EPSPs and dynamically limiting the degree of voltage-dependent Mg^{2+} unblock of NMDAr and NMDAr-dependent Ca^{2+} influx that is important for synaptic plasticity. Moreover, in CA1 pyramidal neurons, the SK2 channel contribution to EPSPs is abolished following the induction of LTP as a result of PKA-dependent phosphorylation, likely occurring at three consecutive serine residues in the intracellular C-terminal domain of SK2 channels. This leads to internalization of spine SK2 channels, thereby contributing together with increased AMPAr function to the increased EPSP that underlies LTP (Lin et al., 2008). Interestingly, CK2 and CaM also interact with NMDAr and alter their properties (Lieberman and Mody, 1999; Krupp et al., 1999; Chung et al., 2004). Given the close spatial arrangement of NMDAr and SK2 channels within the PSD (lin et al., 2008), in response to transmitter initiated intracellular signals CK2 may serve to coordinately tune the activities of these two important and interactive synaptic channels. Therefore, transmitter mediated modulation of the SK2 channel effective Ca^{2+} sensitivity via CK2 may profoundly affect dendritic integration, synaptic responses and synaptic plasticity.

Experimental procedures

Preparation of cell cultures and intranuclear cDNA microinjection

All animals were used in accordance with the European Community guiding in the care and use of animals (86/609/CEE). Primary cultures of rat SCG and DRG neurons and intranuclear microinjection of plasmids were as described (Delmas et al., 2002; Coste et al., 2007; Maingret et al., 2008).

cDNAs and chemicals

Rat Cav2.3, CaM, flag-epitope tagged KCNQ2 and WT and mutant SK2 cDNAs were subcloned into the eukaryotic expression vector pcDNA3. The HA-tagged CK2β, CK2α and CK2αK68M cDNAs were subcloned in pRc/CMV vectors and described previously (Penner

et al., 1997). TBB was obtained from Calbiochem, and all other drugs were from Sigma. Transfection of fetal SCG neurons were performed with Lipofectamine 2000 (Invitrogen) and cells were studied 48–72 hr after transfection.

Perforated microvesicles

The bath solution for recording perforated microvesicles consisted of: NMG^+ 105 mM, $CaCl_2$ 20 mM, KCl 10 mM, $MgCl_2$ 1.2 mM, HEPES 10 mM, 4-AP 0.5 mM, charybdotoxin 100 nM, α and β dendrotoxins (300 nM each), TTX 250 nM and glucose 11 mM (pH 7.3). Sylgard-coated pipettes had resistances of 4–8 MΩ when filled with a pipette solution consisting of (mM): K^+ acetate, 110; KCl, 30; Hepes, 10 (adjusted to pH 7.3 with KOH) and ampho-B (0.05–0.07 mg/ml in DMSO). Retracting the pipette after on-cell patch causes a small vesicle of membrane to remain attached to the pipette, which has its extracellular surface exposed to the bath. Note that the tip of the pipette should not be exposed to air, which would cause the vesicle to open.

Single channel currents were recorded with an Axopatch 200B amplifier (Axon Instruments), filtered at 2 KHz and acquired at 20–50 μs intervals. Voltage-independent leak currents were corrected offline by subtracting null current traces. Sweep currents were evoked every 3–6 s. Transitions between open and closed states were detected by setting the threshold at 50 % of the open channel level. The level of inhibition of SK current was unchanged using 2.5 mM $[Ca^{2+}]_o$ instead of 20 mM (n = 4).

Whole cell Ca^{2+} currents

The bath solution contained (mM): NMG^+ 115, $CaCl_2$ 5, KCl 3, $MgCl_2$ 1.2, HEPES 10, 4-AP 0.5 and glucose 11 mM (pH 7.3). For recording of Ca^{2+} currents in SCG neurons pipettes had resistances of 3–3.5 MΩ and filled with (in mM): CsCl, 30; Cs acetate, 110; $MgCl_2$, 1 and Hepes, 10 (pH 7.3 with CsOH) and 0.1 mg/ml ampho-B. For recording of DRG neurons, pipettes had resistances of 2 MΩ and filled with (in mM): 109 NMDG, 14 CsCl, 10 Hepes, 11 EGTA, 1 $CaCl_2$, 0.1 phosphocreatine, 4 MgATP and 0.2 Na_3GTP (pH 7.3). Cell membrane capacitance and series resistance compensations were applied. Currents were corrected for leak and residual capacitive currents using the leak subtraction procedure (P/6) of pCLAMP8 software.

Whole-cell AHP and I_{AHP}

The bath solution contained (mM): NaCl 140, $CaCl_2$ 2, KCl 3, $MgCl_2$ 1.2, HEPES 10 and glucose 11 (pH 7.3 with NaOH). The internal solution consisted of (mM): K^+ acetate, 90; KCl, 40, Hepes, 20 and $MgCl_2$, 1.2 (pH 7.3 with KOH) and 0.02 mg/ml ampho-B.

Immunoprecipitation

Cultured SCG neurons were harvested and lysed in Tris buffer (50 mM Tris-HCl, 200 mM NaCl, 20 mM NaF, 1 mM Na_3VO_4, 0.5 % Triton X-100, pH 7.4) and complete protease inhibitor cocktail (Roche Diagnostics). The cell lysate was incubated at 4°C overnight with either of the following antibodies: rabbit anti-CaM antibody (Invitrogen), polyclonal SK2 antibody raised against residues 538–555 and mouse anti-flag antibody (Invitrogen). After incubation with protein G-Plus agarose (Santa Cruz biotechnology) for 2 hr, the mixture was centrifuged for 10 s and the supernatant was removed. After washing the agarose beads, immunoprecipitated proteins were eluted in 2x Laemmli sample buffer containing 4 % β-mercaptoethanol (30 min, 37 °C) followed by centrigugation. Equal amounts of protein were loaded onto each lane, separated on SDS-8–12 % polyacrylamide gel and transferred to immunoblot polyvinylidene difluoride membrane. The membrane was blocked in 10 % dry milk for 1 hr and incubated with the relevant primary antibody for 2–4 hr. The membrane was

then washed and incubated with the horseradish peroxidase-conjugated IgG (Zymed) for 1hr at room temperature. The signal was detected using an ECL-chemiluminescence method as described in the manufacturer's protocol.

Autoradiography

For metabolic labeling, SCG neurons were serum-deprived for 12 hr and phosphate-deprived for 2 hr. They were then incubated with 100 μCi/ml of carrier-free [^{32}P]orthophosphoric acid ([$^{32}P_i$]) (900 Ci/mmol) in minimal essential culture medium for 4 hr at 37 °C. When indicated, TBB and calphostin were added to the culture medium for 1 hr. Subsequently, the cells were stimulated at 37 °C with NE. After phosphate-buffered saline washes, the reaction was stopped with 10 % (w/v) trichloroacetic acid. Cells were then harvested and immunoprecipitation was processed as above. Immunopellets were suspended in SDS sample buffer, resolved by SDS-PAGE (8–12 %) and assayed for ^{32}P radioactivity by phosphorimaging.

Statistics and analysis

The $[Ca^{2+}]_i$-p_o curves were fitted with the Hill equation of the form $Y = Y_{max}[Ca^{2+}]_i{}^{nH}/(EC_{50}{}^{nH} + [Ca^{2+}]_i{}^{nH})$, where Y is the normalized p_o, EC_{50} the concentration of Ca^{2+} that produces half-maximal activation of SK channels and n_H the Hill coefficient. The amount of $CaCl_2$ and EGTA in the patch pipette required to yield the free $[Ca^{2+}]_i$ indicated (0.1–10 μM) was calculated as described (Fabiato and Fabiato, 1979). Results are presented as mean ± S.E.M. of *n* experiments. Statistical comparisons were analyzed using Student's *t* test or ANOVA and $P < 0.05$ was considered statistically significant. All experiments were made at room temperature.

Supplementary Material

Refer to Web version on PubMed Central for supplementary material.

Acknowledgements

We would like to thank Prof. David A. Brown for valuable comments on an early version of this manuscript, Prof. B. Hille, K. Mackie, G.W.J. Moss, A.C. Dolphin and F.C. Abogadie for cDNAs and Drs M. Ruzzene and L.A. Pinna for the gift of MNA and NBC compounds. This study was supported by the CNRS and by grants from the Agence Nationale de la Recherche (ANR-05-Neuro-031, ANR-05-PCOD), Fondation Schlumberger, ARCInca-2006, Action Concertée Incitative Jeunes Chercheurs, UPSA, Equipe Fondation pour la Recherche Médicale 2007 and French Ministry (to P.D.) and by grants from NIH NRSA Award (to D.A.) and NIH (to J.P.A.).

References

Allen D, Fakler B, Maylie J, Adelman JP. Organization and regulation of small conductance Ca^{2+}-activated K^+ channel multiprotein complexes. J. Neurosci 2007;27:2369–2376. [PubMed: 17329434]

Arrigoni G, Marin O, Pagano MA, Settimo L, Paolin B, Meggio F, Pinna LA. Phosphorylation of calmodulin fragments by protein kinase CK2. Mechanistic aspects and structural consequences. Biochemistry 2004;43:12788–12798. [PubMed: 15461451]

Bahia PK, Suzuki R, Benton DC, Jowett AJ, Chen MX, Trezise DJ, Dickenson AH, Moss GW. A functional role for small-conductance calcium-activated potassium channels in sensory pathways including nociceptive processes. J Neurosci 2005;25:3489–3498. [PubMed: 15814779]

Bildl W, et al. Protein kinase CK2 is coassembled with small conductance Ca_{2+}- activated K_+ channels and regulates channel gating. Neuron 2004;43:847–858. [PubMed: 15363395]

Bond CT, Herson PS, Strassmaier T, Hammond R, Stackman R, Maylie J, Adelman JP. Small conductance Ca^{2+}-activated K^+ channel knock-out mice reveal the identity of calcium-dependent afterhyperpolarization currents. J Neurosci 2004;24:5301–5306. [PubMed: 15190101]

Bond CT, Maylie J, Adelman JP. Small-conductance calcium-activated potassium channels. Ann. N. Y. Acad. Sci 1999;868:370–378. [PubMed: 10414306]

Bond CT, Maylie J, Adelman JP. SK channels in excitability, pacemaking and synaptic integration. Curr. Opin. Neurobiol 2005;15:305–311. [PubMed: 15922588]

Bourinet E, Soong TW, Stea A, Snutch TP. Determinants of the G protein-dependent opioid modulation of neuronal calcium channels. Proc. Natl. Acad. Sci. USA 1996;93:1486–1491. [PubMed: 8643659]

Cai X, Liang CW, Muralidharan S, Kao JP, Tang CM, Thompson SM. Unique roles of SK and Kv4.2 potassium channels in dendritic integration. Neuron 2004;44:351–364. [PubMed: 15473972]

Chung HJ, Huang YH, Lau LF, Huganir RL. Regulation of the NMDA receptor complex and trafficking by activity-dependent phosphorylation of the NR2B subunit PDZ ligand. J Neurosci 2004;24:10284–10259.

Coste B, Crest M, Delmas P. Pharmacological dissection and distribution of NaN/Nav1.9, T-type Ca_{2+} currents, and mechanically activated cation currents in different populations of DRG neurons. J Gen Physiol 2007;129:57–77. [PubMed: 17190903]

Delmas P, Abogadie Fe, C, Buckley NJ, Brown DA. Calcium channel gating and modulation by transmitters depend on cellular compartmentalization. Nature Neurosci 2000;3:670–678. [PubMed: 10862699]

Delmas P, Brown DA. Junctional signaling microdomains: bridging the gap between the neuronal cell surface and Ca_{2+} stores. Neuron 2002;36:787–790. [PubMed: 12467583]

Delmas P, Brown DA. Pathways modulating neural KCNQ/M (Kv7) potassium channels. Nature Rev Neurosci 2005;6:850–862. [PubMed: 16261179]

Delmas P, Wanaverbecq N, Abogadie FC, Mistry M, Brown DA. Signaling microdomains define the specificity of receptor-mediated InsP3 pathways in neurons. Neuron 2002;34:209–220. [PubMed: 11970863]

Dreixler JC, Bian J-T, Cao Y-J, Roberts MT, Roizen JD, Houamed KM. Block of rat brain recombinant SK channels by tricyclic antidepressants and related compounds. Eur. J. Pharmacol 2000;401:1–7. [PubMed: 10915830]

Faber ES, Delaney AJ, Sah P. SK channels regulate excitatory synaptic transmission and plasticity in the lateral amygdala. Nat Neurosci 2005;8:635–641. [PubMed: 15852010]

Faber ES, Sah P. Functions of SK channels in central neurons. Clin Exp Pharmacol Physiol 2007;34:1077–1083. [PubMed: 17714097]

Fabiato A, Fabiato F. Calculator programs for computing the composition of the solutions containing multiple metals and ligands used for experiments in skinned muscle cells. J. Physiol. (Paris) 1979;75:463–505. [PubMed: 533865]

Galarraga E, et al. Somatostatinergic modulation of firing pattern and calcium-activated potassium currents in medium spiny neostriatal neurons. Neuroscience 2007;146:537–554. [PubMed: 17324523]

Gamper N, Shapiro MS. Calmodulin mediates Ca^{2+}-dependent modulation of M-type K_+ channels. J Gen Physiol 2003;122:17–31. [PubMed: 12810850]

Gu N, Vervaeke K, Hu H, Storm JF. Kv7/KCNQ/M and HCN/h, but not KCa_2/SK channels, contribute to the somatic medium after-hyperpolarization and excitability control in CA1 hippocampal pyramidal cells. J. Physiol 2005;566:689–715. [PubMed: 15890705]

Hammond RS, Bond CT, Strassmaier T, Ngo-Anh TJ, Adelman JP, Maylie J, Stackman RW. Small-conductance Ca_{2+}-activated K^+ channel type 2 (SK2) modulates hippocampal learning, memory, and synaptic plasticity. J. Neurosci 2006;26:1844–1853. [PubMed: 16467533]

Hirschberg B, Maylie J, Adelman JP, Marrion NV. Gating of recombinant small-conductance Ca-activated K^+ channels by calcium. J. Gen. Physiol 1998;111:571–581.

Hosseini R, Benton DCH, Dunn PM, Jenkinson DH, Moss GWJ. SK3 is an important component of K $^+$ channels mediating the afterhyperpolarization in cultured rat SCG neurones. J. Physiol. (Lond.) 2001;535:323–334. [PubMed: 11533126]

Ikeda SR. Voltage-dependent modulation of N-type calcium channels by G-protein beta gamma subunits. Nature 1996;380:255–258. [PubMed: 8637575]

Keen JE, et al. Domains responsible for constitutive and Ca^{2+}-dependent interactions between calmodulin and small conductance Ca^{2+}-activated potassium channels. J. Neurosci 1999;19:8830–8838. [PubMed: 10516302]

Köhler M, et al. Small-conductance, calcium-activated potassium channels from mammalian brain. Science 1996;273:1709–1714. [PubMed: 8781233]

Krupp JJ, Vissel B, Thomas CG, Heinemann SF, Westbrook GL. Interactions of calmodulin and alpha-actinin with the NR1 subunit modulate Ca^{2+}-dependent inactivation of NMDA receptors. J Neurosci 1999;19:1165–1178. [PubMed: 9952395]

Lieberman DN, Mody I. Casein kinase-II regulates NMDA channel function in hippocampal neurons. Nat Neurosci 1999;2:125–132. [PubMed: 10195195]

Lin MT, Luján R, Watanabe M, Adelman JP, Maylie J. SK2 channel plasticity contributes to LTP at Schaffer collateral-CA1 synapses. Nat Neurosci 2008;11:170–177. [PubMed: 18204442]

Litchfield DW. Protein kinase CK2: structure, regulation and role in cellular decisions of life and death. Biochem. J 2005;369:1–15. [PubMed: 12396231]

Martina M, Turcotte M-EB, Halman S, Bergeron R. The sigma-1 receptor modulates NMDA receptor synaptic transmission and plasticity via SK channels in rat hippocampus. J. Physiol 2007;578:143–157. [PubMed: 17068104]

Maingret F, Coste B, Padilla F, Clerc N, Crest M, Korogod SM, Delmas P. Inflammatory mediators increase Nav1.9 current and excitability in nociceptors through a coincident detection mechanism. J Gen Physiol 2008;131:211–225. [PubMed: 18270172]

Maylie J, Bond CT, Herson PS, Lee W-S, Adelman JP. Small conductance Ca^{2+}-activated K^+ channels and calmodulin. J. Physiol 2003;554:255–261. [PubMed: 14500775]

Meggio F, et al. Inhibition of protein kinase CK2 by condensed polyphenolic derivatives. An in vitro and in vivo study. Biochemistry 2004;43:12931–12936. [PubMed: 15461466]

Monaghan AS, Benton DCH, Bahia PK, Hosseini R, Shah YA, Haylet DG, Moss GWJ. The SK3 subunit of small conductance Ca^{2+}-activated K^+ channels interacts with both SK1 and SK2 subunits in a heterologous expression system. J. Biol. Chem 2004;279:1003–1009. [PubMed: 14559917]

Mongan LC, Hill MJ, Chen MX, Tate SN, Collins SD, Buckby L, Grubb BD. The distribution of small and intermediate conductance calcium-activated potassium channels in the rat sensory nervous system. Neuroscience 2005;131:161–175. [PubMed: 15680700]

Ngo-Anh TJ, Bloodgood BL, Lin M, Sabatini BL, Maylie J, Adelman JP. SK channels and NMDA receptors form a Ca^{2+} -mediated feedback loop in dendritic spines. Nat Neurosci 2005;8:642–649. [PubMed: 15852011]

Page KM, Cantí C, Stephens GJ, Berrow NS, Dolphin AC. Identification of the amino terminus of neuronal Ca^{2+} channel alpha1 subunits alpha1B and alpha1E as an essential determinant of G-protein modulation. J. Neurosci 1998;18:4815–4824. [PubMed: 9634547]

Pertovaara A. Noradrenergic pain modulation. Prog. in Neurobiol 2006;80:53–83.

Penner CG, Wang ZL, Litchfield DW. Expression and localization of epitope-tagged protein kinase CK2. J. Cell Biochem 1997;64:525–537. [PubMed: 9093902]

Stackman RW, Hammond RS, Linardatos E, Gerlach A, Maylie J, Adelman JP, Tzounopoulos T. Small conductance Ca^{2+}-activated K^+ channels modulate synaptic plasticity and memory encoding. J. Neurosci 2002;22:10163–10171. [PubMed: 12451117]

Stocker M, Krause M, Pedarzani P. An apamin-sensitive Ca^{2+}-activated K^+ Proc Natl Acad Sci USA 1999;96:4662–4467. [PubMed: 10200319]

Storm JF. Potassium currents in hippocampal pyramidal cells. Prog. Brain Res 1990;83:161–187. [PubMed: 2203097]

Strassmaier T, Bond CT, Sailer CA, Knaus HG, Maylie J, Adelman JP. A novel isoform of SK2 assembles with other SK subunits in mouse brain. J Biol Chem 2005;280:21231–21236. [PubMed: 15797870]

Vilk G, Saulnier RB, St Pierre R, Litchfield DW. Inducible expression of protein kinase CK2 in mammalian cells. Evidence for functional specialization of CK2 isoforms. J. Biol. Chem 1999;274:14406–14414. [PubMed: 10318865]

Wagner EJ, Rønnekleiv OK, Kelly MJ. The noradrenergic inhibition of an apamin-sensitive, small-conductance Ca^{2+}-activated K^+ channel in hypothalamic gamma-aminobutyric acid neurons: pharmacology, estrogen sensitivity, and relevance to the control of the reproductive axis. J. Pharmacol. Exp. Ther 2001;299:21–30. [PubMed: 11561059]

Wen H, Levitan IB. Calmodulin is an auxiliary subunit of KCNQ2/3 potassium channels. J. Neurosci 2002;22:7991–8001. [PubMed: 12223552]

Xia X-M, et al. Mechanism of calcium gating in small-conductance calcium-activated potassium channels. Nature 1998;395:503–507. [PubMed: 9774106]

Yus-Nájera E, Santana-Castro I, Villarroel A. The identification and characterization of a noncontinuous calmodulin-binding site in noninacticating voltage-dependent KCNQ potassium channels. J. Biol. Chem 2002;277:28545–28553. [PubMed: 12032157]

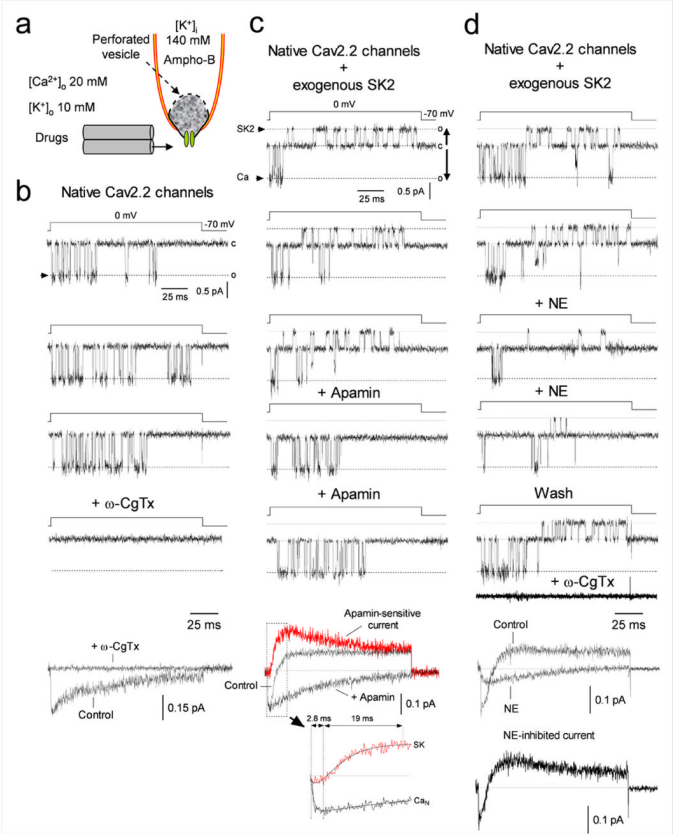

Fig. 1. Coupling activity and concurrent inhibition of Cav2.2 and SK channels

(**a**) Schematic diagram of an outside-out perforated microvesicle using amphotericin B in the patch pipette (see methods).

(**b**) Activation of a Cav2.2 channel (16.3 pS) in the absence or presence of ω-CgTx GVIA (500 nM). Bottom traces represent ensemble currents averaged from 92 (control) and 37 (ω-CgTx GVIA) consecutive single channel sweeps (including nulls).

(**c–d**) Two different perforated microvesicles pulled-out from 2 different neurons overexpressing rSK2 subunits. (**c**) Simultaneous activation of a Cav2.2 channel (17.3pS) and an apamin-sensitive SK channel (8.2 pS). Bottom traces: corresponding ensemble-averaged currents in the absence (78 sweeps) or presence (47 sweeps) ofapamin (300 nM). Red trace: isolated SK current. Inset: kinetics of activation of native Cav2.2 and SK channels were extended at fast time resolution. The times indicated represent *onset to onset* and *peak to peak* of the currents. (**d**) As in (**c**) but in the presence or absence of NE (1 μM) and of ω-CgTx GVIA (500 nM). Bottom traces: shown are ensemble-averaged currents with and without NE (60 sweeps each) and NE-inhibited current (difference current). Experiments made in the continued presence of 4-AP (0.5 mM), charybdotoxin (100 nM), α and β dendrotoxins (300 nM each) and TTX 250 nM.

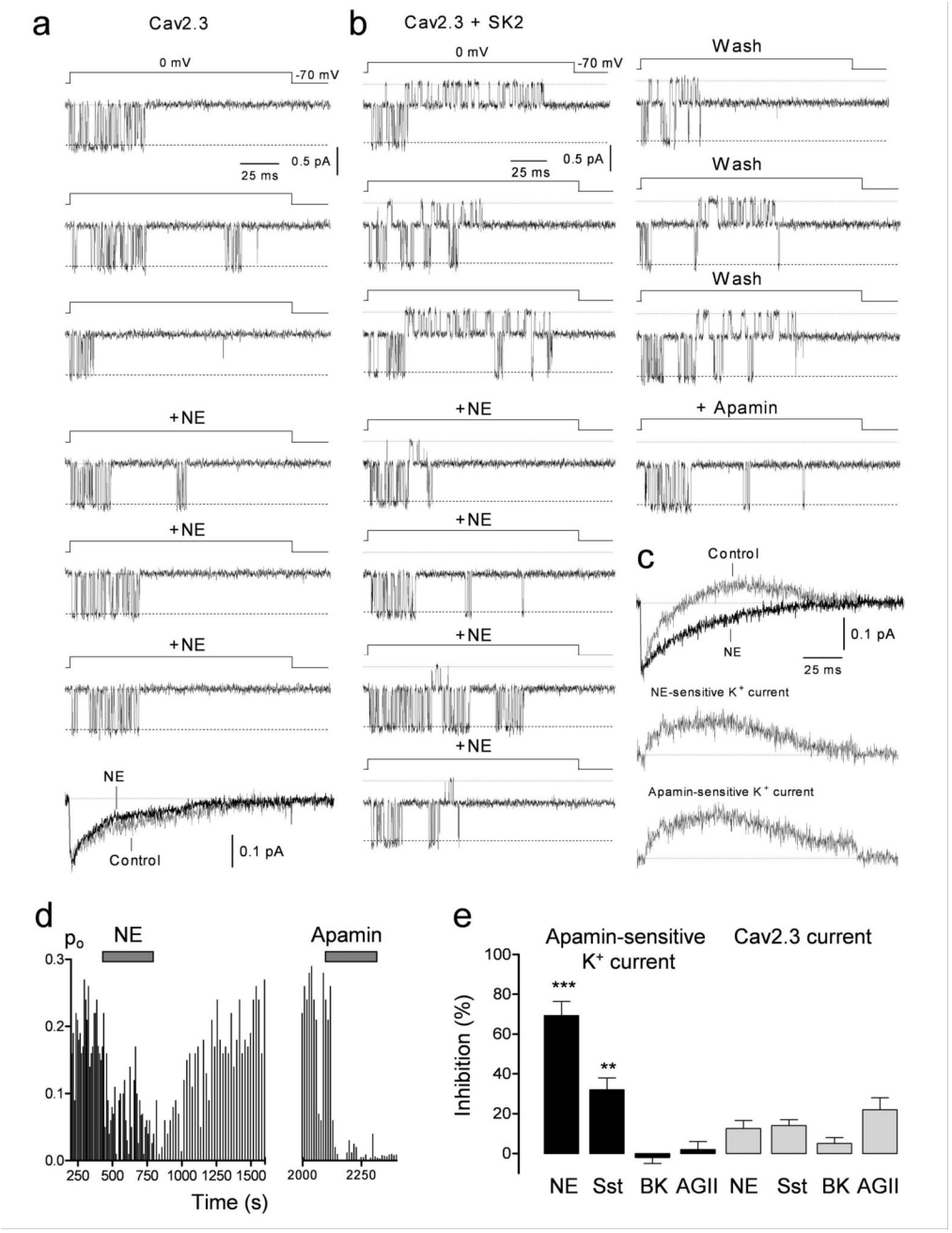

Fig. 2. SK channels, but not priming Ca2.3 channels, are inhibited by neurotransmitters

(a–e) Recording conditions were as in Fig. 1, except that ω-CgTx GVIA (500 nM) and nifedipine (1 μM) were present throughout. (**a**) Neuron expressing Cav2.3 channels. Activation of a Cav2.3 channel (~15 pS) in the absence and presence of NE (1 μM). Bottom traces: corresponding ensemble currents averaged from 72 (control) and 80 (NE) consecutive single channel sweeps.

(**b–d**) Data from the same microvesicle excised from a neuron expressing Cav2.3 and SK2 channels. (**b**) Activities of a Cav2.3 channel (~15.3 pS) and a SK channel (7.9 pS) in the presence or absence of NE (1 μM), after washing out NE and in the presence of apamin (300 nM). (**c**) Corresponding ensemble-averaged currents in the presence (72 sweeps, ~3.5 min) and absence (89 sweeps) of NE. Bottom traces: NE-sensitive K^+ current and K^+ component

blocked by apamin. Note their similar shape. (**d**) Open probability (p_o) *versus* time from the SK channel shown in **b**. p_o was averaged from 3 successive single channel sweeps (including nulls).

(**e**) Summary of the effects of NE (1 μM, n = 7), Sst (500 nM, n = 8), BK (200 nM, n = 6) and AGII (500 nM, n = 5) on the apamin-sensitive K^+ current (black bars) and on the Cav2.3 current (grey bars). Inhibition was measured from ensemble currents as in **c**. **, $P < 0.01$; ***, $P < 0.001$, relative to BK and AGII applications.

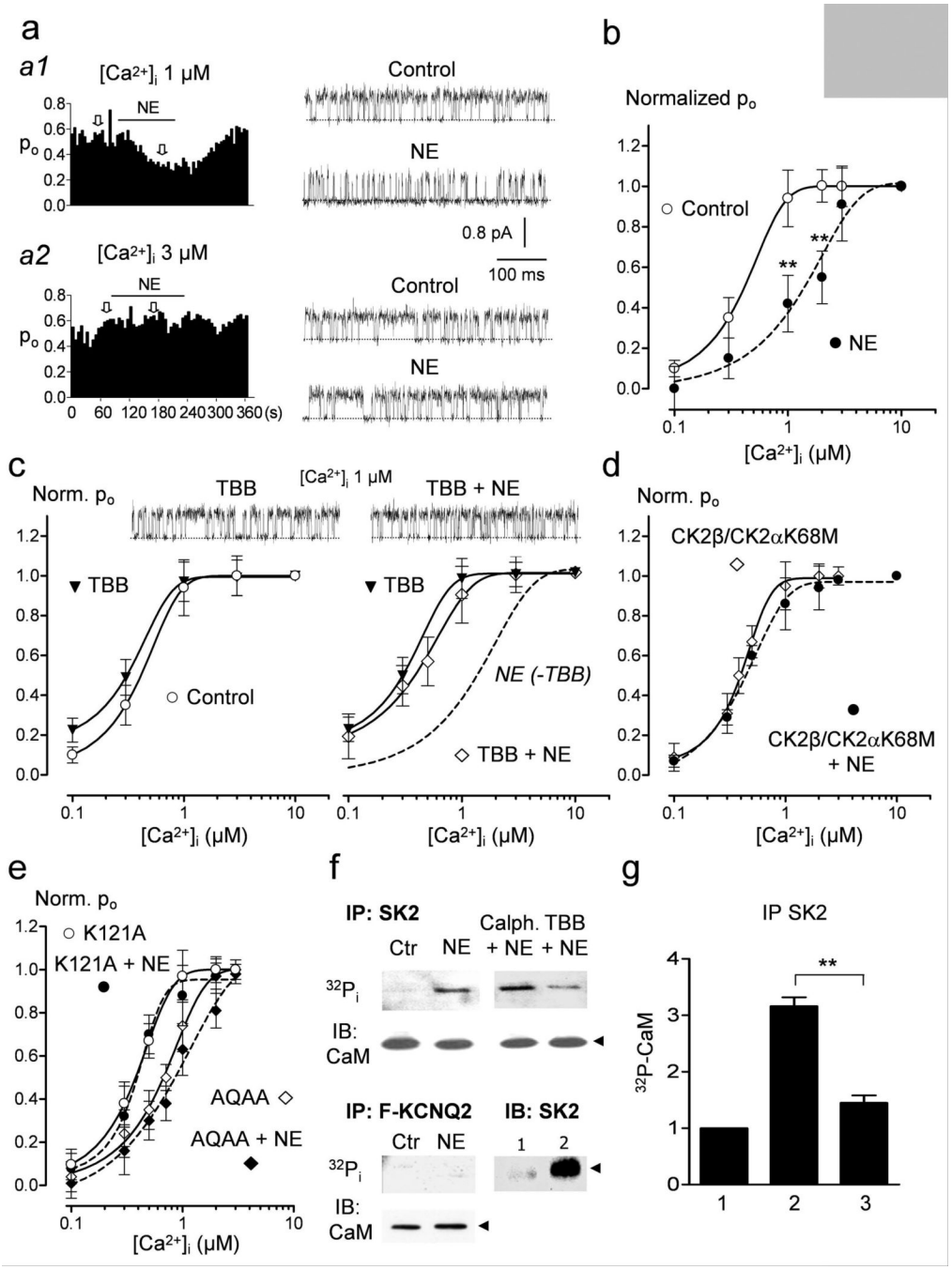

Fig. 3. Transmitter inhibition of SK channels via reduced Ca^{2+} sensitivity of channel gating

(**a**) Left panels: shown are SK p_o plotted against time in perforated microvesicles loaded with either 3 µM (**a1**) or 1 µM (**a2**) free Ca^{2+} in the presence or absence of NE (1 µM). p_o was calculated from 6 s-periods during 360 s-recording. V_h = +5 mV. Right panels: corresponding activities of single SK channels collected at the time indicated by arrows.

(**b**) Steady-state Ca^{2+} response relationships for SK channels in the absence (○) or presence (●) of NE (1 µM). Relative p_o was measured at +5 mV and was plotted as a function of $[Ca^{2+}]_i$. Experiments obtained as in (**a**). Data points are the mean ± S.E.M. with 5–8 experiments per Ca^{2+} concentration. Solid lines represent best fits of a single Hill equation,

giving EC_{50} of 0.42 ± 0.06 and 1.37 ± 0.1 μM for control and NE conditions, respectively. **, $P < 0.01$.

(**c**) Left panel: steady-state Ca^{2+} response relationships for SK channels in the absence (○, data from **b**) or presence (▼) of TBB (10 μM, 1 hr pre-treatment). Hill equations yield EC_{50} of 0.40 ± 0.05 and 0.31 ± 0.08 μM, respectively (n = 4–8). Right panel: the effect of NE application on Ca^{2+} response relationships for SK channels exposed to TBB (◊, n = 6). EC_{50} was 0.39 ± 0.09 μM. The dashed line represents the Ca^{2+} response relationship for SK channels exposed to NE in the absence of TBB (data from panel **b**). The top traces illustrate single SK channel activities obtained with 1 μM $[Ca^{2+}]_i$ in TBB-treated vesicles with and without NE. Scale as in (**a**).

(**d**) Steady-state Ca^{2+} response relationships for SK channels from neurons expressing CK2β/CK2αK68M, in the presence (●, n = 11) or absence (◊, n = 13) of NE. The respective EC_{50} values were 0.43 ± 0.07 and 0.38 ± 0.08 μM.

(**e**) Steady-state Ca^{2+} response relationships for SK channels from neurons expressing K121A (○) and AQAA (◊) SK2 mutants, in the absence (open symbols) or presence (filled symbols) of NE. EC_{50} values were 0.36 ± 0.08 (n = 6) and 0.71 ± 0.05 μM (n = 5) for K121A and AQAA mutants in the absence of NE and 0.39 ± 0.09 (n = 5) and 0.98 ± 0.09 μM (n = 5) in the presence of NE, respectively.

(**f**) Upper panel: autoradiograph and immunoblot of SK2 immunoprecipited from transfected fetal SCG neurons. CaM phosphorylation level was tested with and without NE (1 μM, 30 min) in cells pre-treated with 10 μM TBB or calphostin (Calph., 200 nM), an inhibitor of PKC, for 1 hr. The arrow indicates the expected size of CaM (~17 kDa). Lower panel: autoradiograph and immunoblot of flag-KCNQ2 immunoprecipited from transfected fetal SCG neurons (left panel). CaM phosphorylation level was tested with and without NE (1 μM, 30 min). Shown on the right is a western blot with the SK2 antibody performed on whole cell lysates prepared from cells transfected (2) or not (1) with SK2 cDNA. The arrow indicates the expected size of SK2 (~50 kDa).

(**g**) Quantification of the incorporation of ^{32}P into SK2-bound CaM. Densitometric analysis was made from experiments as in **f**, plotting the change in the ^{32}P-CaM signal relative to the signal obtained for CaM labeling in control cells (set to 1). Cells were treated as follows: 1, Control; 2, NE for 30 min; 3, TBB applied for 1 hr and NE applied for 30 min before cell lysis. **, $P < 0.01$.

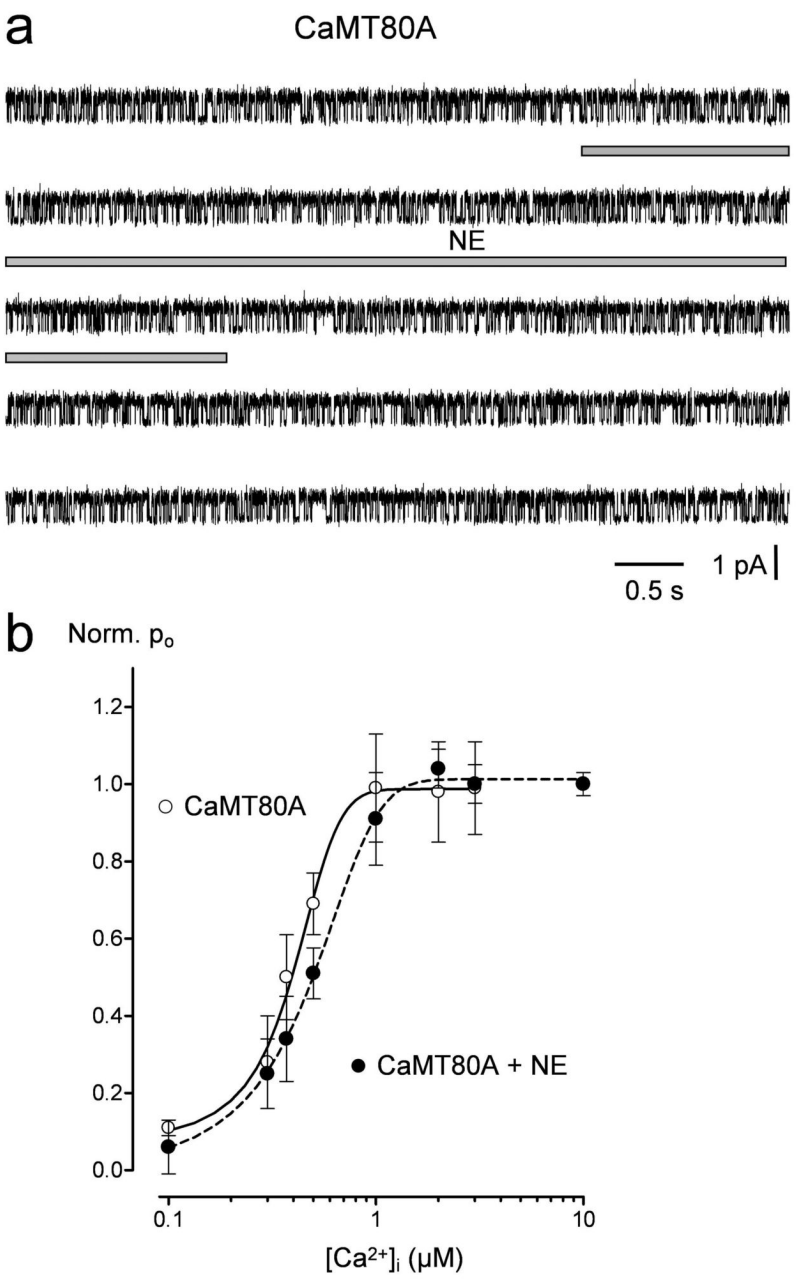

Fig. 4. Reduced modulation of CaMT80A-associated SK channels

(**a**), Activity of a CaMT80A-bound SK channel in the absence or presence of NE (1 μM) collected in a microvesicle loaded with 1 μM free Ca^{2+}. Sweeps were separated by 60 s. (**b**) Steady-state Ca^{2+} response relationships for SK channels in the absence (○) or presence (●) of NE (1 μM). Relative p_o was measured at +5 mV and was plotted as a function of $[Ca^{2+}]_i$. Solid lines represent best fits of a single Hill equation, giving EC_{50} of 0.37 ± 0.08 and 0.45 ± 0.09 μM (n = 7) for control and NE conditions, respectively. $P > 0.05$.

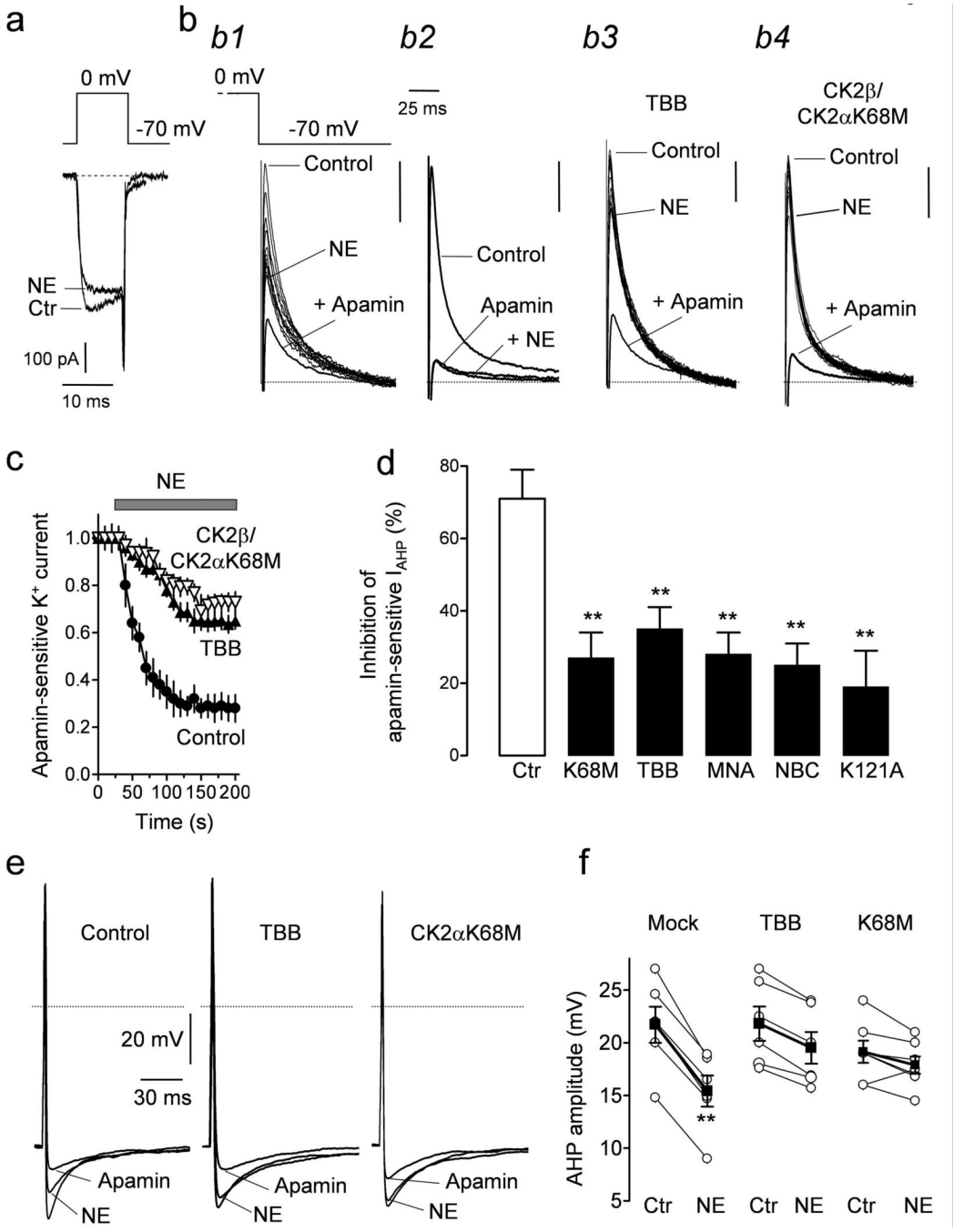

Fig. 5. Transmitter inhibition of SK channel-mediated AHP involves CK2

(**a-f**) Neurons expressing rCav2.3 and SK2. (**a**) The effects of NE (1 μM) on whole-cell Ca^{2+} currents, primarily made up of Cav2.3, evoked by a 10 ms-test pulse to 0 mV. Recordings were made using the perforated patch configuration with a CsCl-based pipette solution and in the continued presence of ω-CgTx GVIA (250 nM), nifedipine (1 μM) and TTX (250 nM). (**b**) Whole cell I_{AHP} was measured using the perforated patch configuration using a KAc/KCl-based internal solution in response to 20 ms-depolarizing voltage pulse to 0 mV. In addition to ω-CgTx GVIA, nifedipine and TTX, linopirdine (10 μM) was added to the bath solution to suppress KCNQ/M tail current. NE-induced I_{AHP} inhibition before (**b1**) and after (**b2**) apamin (100 nM) application. NE inhibition in a neuron pre-treated with TBB (10 μM for 1 hr) (**b3**)

and in a neuron expressing CK2β/CK2αK68M (**b4**). Currents were evoked every 10 s; 13 superimposed traces are shown in each panel. Scale bars: 100 pA.
(**c**) Inhibition of apamin-sensitive peak I_{AHP} obtained from experiments as in **b**, depicted as a function of time (n = 5–8 cells).
(**d**) Graph summarizing NE-mediated inhibition of the apamin-sensitive I_{AHP} in control neurons (Ctr, n = 8), in CK2β/CK2αK68M-expressing neurons (K68M, n = 6), in neurons pre-treated for 1 hr with TBB (10 μM, n = 5), MNA and NBC (1 μM, n = 5) and in neurons expressing the SK2 K121A mutant. **, $P < 0.01$ respective to control.
(**e,f**) ω-CgTx GVIA (250 nM) and nifedipine (1 μM) throughout, no linopirdine added. (**e**) Single action potentials evoked by brief pulses (5 ms) showing reduced NE-mediated AHP inhibition in neurons treated with TBB (10 μM) or expressing CK2β/CK2αK68M. Apamin (200 nM) was added at the end of each experiment. (**f**) Plot showing the effect of NE on AHP amplitude in each individual cell (open symbols) for these 3 groups. Black symbols indicate averaged results (**, $P < 0.01$, paired *t*-test).

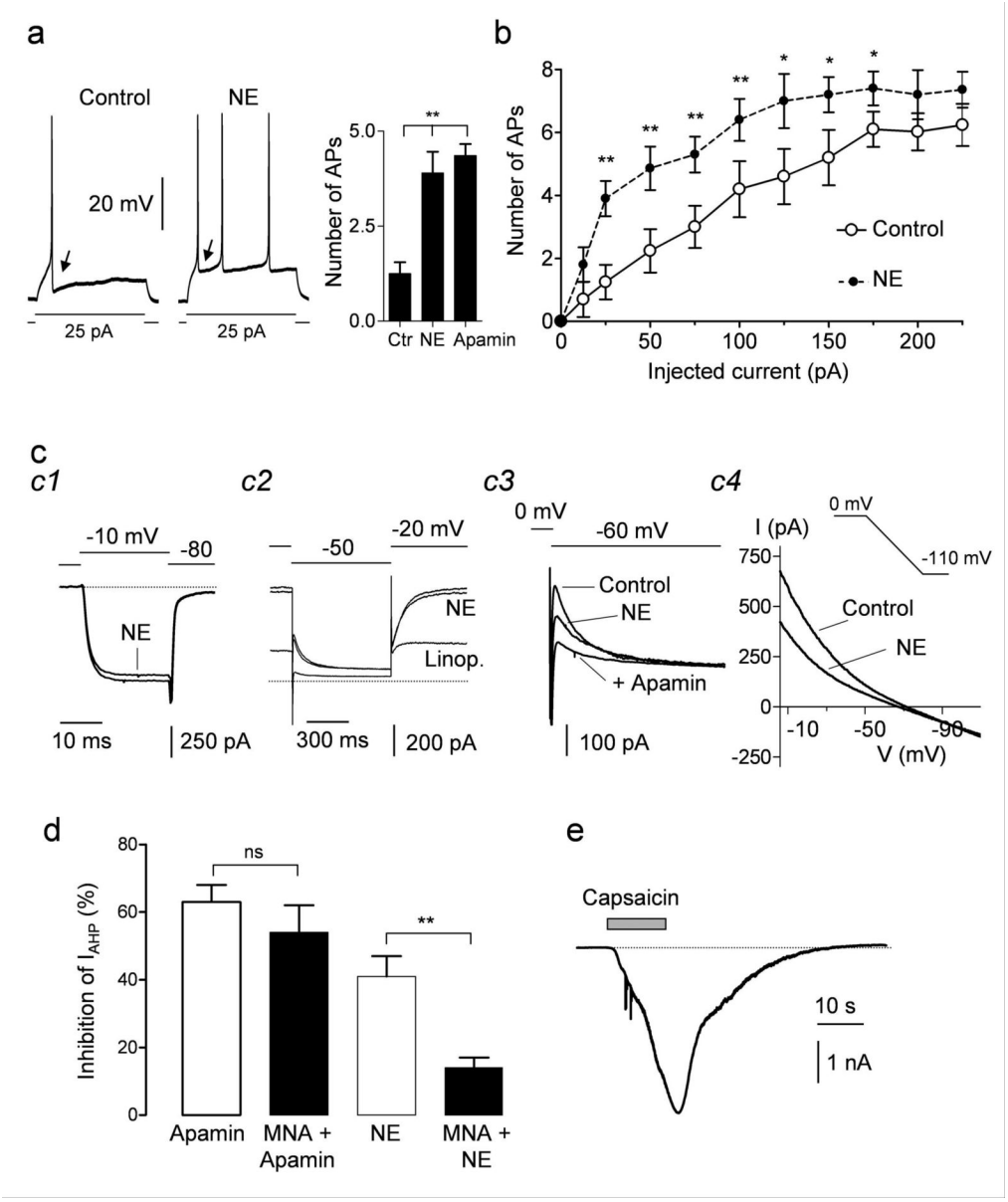

Figure 6. Inhibition of native SK current increases the somatic excitability of small sensory neurons

(**a–c**), Cultured DRG neurons were bathed with ω-CgTx GVIA (200 nM), nifedipine (1 μM), ω-agatoxin IVA (200 nM) and amiloride (250 μM).

(**a**), A small DRG neuron (37 pF) was studied under perforated patch current clamp, and voltage responses were recorded from a 25 pA current pulse applied for 400 ms. Voltage sweeps are shown before or after 1.5 min application of NE (10 μM). Note that AHP was strongly suppressed by NE (arrows). Right panel: histogram showing the number of APs (mean ± SEM, n = 8) elicited during a 400 ms-duration 25 pA-current pulse in control (1) and in the presence of either NE (2) or apamin (300 nM, 3). (**b**), Number of APs (mean ± SEM) evoked during 400 ms-current pulses versus amplitude of injected currents in the absence (○) or presence (●) of NE. (**c**), Recording of Cav2.3 current (**c1**, patch ruptured), native KCNQ/M K^+ current (**c2**, perforated patch) and native SK current (**c3**,**4**, perforated patch) in small DRG neurons in the presence or absence of NE. Linop.: linopirdine 10 μM; Apamin, 300 nM. In **c4** the ramp speed was - 100 mV/s. (**d**) Graph summarizing apamin and NE-mediated inhibitions of I_{AHP}

evoked as in **c3** in DRG neurons pretreated or not with MNA (1 μM). n = 5–7; **, $P < 0.01$; ns, not significant. (**e**), Capsaicin (1 μM)-induced TRPV1 inward current in the cell illustrated in **a**. Holding potential, −60 mV.